OPEN ACCESS

Kashf Journal of Multidisciplinary Research
Vol: 02 - Issue 2 (2025)
P-ISSN: 3007-1992 E-ISSN: 3007-200X
https://kjmr.com.pk

Investigating the Effects of Cerium Doping on the Chemical and Optical Properties of Lanthanum Phosphate Nanoparticles

Muhammad Salman
Faculty of Sciences, The Superior University, Lahore salmanmsc2014@gmail.com
Zeeshan Mahmood
Faculty of Sciences, The Superior University, Lahore
Aurangzaib
Faculty of Sciences, The Superior University, Lahore
Kanwal Akhtar
Faculty of Sciences, The Superior University, Lahore
Aneela Din Muhammad
Faculty of Sciences, The Superior University, Lahore
Waseem Sajjad Tahir
Faculty of Sciences, The Superior University, Lahore
Muhammad Iqbal
Faculty of Sciences, The Superior University, Lahore
Yasir Javeed
Department of Physics, University of Agriculture, Faisalabad, Pakistan

Corresponding author:

DOI: *https://doi.org/10.71146/kjmr264*

Article Info

Abstract

Synthesis of cerium doped lanthanum phosphate nanoparticles is described here by simple co-precipitation technique. The phase, morphology and composition 2.0 mol% Ce and 6.0 mol% Ce doped lanthanum phosphate were analyzed by Fourier transform infrared spectroscopy (FTIR) and UV-visible spectroscopy. Fourier transform infrared spectroscopy (FTIR) confirms the water vibration modes at a specific wave number along with a phosphate group and variation in wave numbers when cerium is incorporated in to lanthanum phosphate. Infrared spectral data presented for the produced sample were recorded on a Fourier transform spectrometer with the scan range of 650-4000 cm^{-1}. For the excitation and monitor photoluminescence (PL), the spectra as well as the PL were also obtained. Luminescent Co_3^+ doped $LaPO_4$ when synthesized at 2.0 and 6.0 mole % was seen to exhibit PL emission. UV spectroscopic analyses show that the present absorption bands are located in the ultraviolet region and noticeably depend on the presence of dopant ions. The created samples can be sued in various lighting and display application devices.

Keywords:
Co-Precipitation, UV-Visible spectroscopy, FTIR, Photoluminescence, Display devices

Introduction

Inorganic nanoparticles are synthesized with much effort because of their commercial application. Owing to their unique morphology and vast application in producing nanoscale displays, sensors, and optoelectronic devices, materials with controlled size and shape have attracted focus [1], [2], [3]. Lighting and display panels are quite common places where phosphors are often used. In fact, one of the most crucial characteristics of phosphors that defines the ability to use them in various applications is their size and shape. Sphere-shaped phosphor particles can help enhance the optical and morphological elements of phosphor layers regarding their composition [4], [5], [6]. To achieve the desired coating for the specific application varies quantity of phosphor particles with the particle size. Thus, much attention has been given to the technique of engineering nanomaterials with desired morphologies. Recently, RE doped nanoscale $LaPO_4$ has become the area of interest due to its application in optoelectronic devices, integrated optical systems, sensitive devices, plasma display panels, and optical display panels and other applications [7], [8], [9] [10]. The application of RE compounds particularly lanthanum phosphate with inorganic dopant has been elaborated as follows. It is challenging to synthesize such materials economically even though there have been improvements in preparation of the materials [1], [2], [11], [12]. Some common phosphors are of the form $LaPO_4$ with lanthanide (Ln) doped phosphors which serve various commercial applications. Among phosphors currently used to boost the brightness and meet the need for developing new types of display panels and devices, some of them have been the focus of much study. LaPO4 doped with rare earth ions was a kind of important phosphate phosphors due to its interesting characters such as high quantum efficiency, good chemical stability, and tunable emission colour with various activators. Several solution-phase techniques have been tried to lower the reaction temperature and synthesise rare earth phosphate-based nanoparticles such as, hydrothermal, sol-gel, combustion, precipitation, water-in-oil microemulsion, polyol-mediated synthesis, and ultrasonic irradiation[6], [12], [13]. In an effort to optimize LaPO4 based nanoparticles, both the reaction time and temperature have been reduced in this case. However, it is still very challenging to control the morphology of $LaPO_4$ and realize the nanoscale synthesis. Based on the present study, the chemical co-precipitation process seems to be the most appropriate and suitable method for controlling particle morphology. Here, a simple chemical co-precipitation technique has been adopted to synthesized Ce:$LaPO_4$ with different concentration of cerium at relatively homogenous size and shape with fine crystals are produced. The following features can be distinguished. The compound has a relatively high thermal stability, and it is poorly soluble in water, however, its index of refraction is rather high. In this paper the photoluminescence (PL) of the Ce:$LaPO_4$ phosphor with different concentration of cerium has been synthesized [8], [13], [14], [15] .

Material synthesis:

The synthesis of lanthanum phosphate ($LaPO_4$) nanoparticles with good morphological control is very difficult. In this context, the best strategy to regulate powder morphology seems to be the chemical approach, especially the co-precipitation method as it means that the components are intimately mixed throughout the process [16] [17]. When compared with this other approaches, some of the advantages include low firing temperature, early stage control of the reaction process and stable elemental composition. Lanthanum phosphate doped form with different ceria concentration (2.0 mol% and 6 mol%) of Lanthanum was synthesized by using lanthanum chloride heptahydrate ($LaCl_3.7H_2O$), potassium dihydrogen phosphate (K_2HPO_4), and cerium (III) nitrate hexahydrate ($CeN_3.6H_2O_3$) [18]. To synthesize pure lanthanum phosphate LaPO4, we use lanthanum chloride heptahydrate ($LaCl_3 \cdot 7H_2O$) in 100 ml and potassium dihydrogen phosphate (K_2HPO_4) in 100 ml of deionized water [19]. Independently, both solutions are then placed onto the magnetic stirrer and let to stir for 30 minutes. Following that, potassium dihydrogen phosphate solution is gradually added into a solution of lanthanum chloride heptahydrate. Finally, stir the final solution for 40 min and leave the solution at room temperature for 24 hours, it will

appear whitish precipitate at the bottom [11] [20] . Wash the sample many times. The thick mass was dried at 80 0C and properly grounded using mortar and pestle for analysis. Characterization of the so prepared powdered sample was subsequently accomplished with the aid of Fourier transform infrared spectroscopy (FTIR) and UV-visible spectroscopy [7].

For preparation of cerium-doped lanthanum phosphate (abbreviated as Ce:LaPO4), the doped ion in the required mole percentage was added to the parent ion, e.g., to prepare 2% cerium-doped lanthanum phosphate 0.01 M solution of CeNO3 was prepared with de-ionized water and then stirred. 0.99 M of LaCl3 with potassium dihydrogen phosphate was prepared in same way. The two solutions were thoroughly mixed [20]. The rest of the phenomenon is same as in case of pure lanthanum phosphate.

Characterization techniques:

The prepared powdered sample was characterized by using Fourier transform infrared spectroscopy (FTIR) and UV-Visible Spectroscopy.

FTIR spectroscopy:

FTIR as an analytical tool for identifying functional groups and covalent bonding data or in other words it determines the chemical structure and the type of chemical bonds and internal structure of a molecule in the grown nanomaterial [21]. Vibrational spectra of 2% Ce:Fig 1.0 (a, b) show the diffractograms for synthesised LaPO4 and 6% Ce: LaPO4.The band gap spectra occurred at lower wave numbers 989.608; 30.809 Cm-1 , 1634.438;86.940 Cm-1 and 3431.014; 87.148 Cm -1 for 2 % Ce doped lanthanum phosphate belong to O=P–O bending, and O–P–O bending vibrations respectively.present in the grown nanomaterial [21]. Vibrational spectra of 2% Ce:LaPO4 and 6% Ce: LaPO4 are shown in Fig 1.0 (a, b) respectively.

In case of 2% Ce doped lanthanum phosphate the band gap spectra appear at 989.608; 30.809 Cm-1 , 1634.438;86.940 Cm-1 and 3431.014; 87.148 Cm-1 correspond to O=P–O bending and O–P–O bending modes, respectively [22]. The weak bands are also observed in wave numbers 3431.014; 87.148 cm-1. These weak bands are due to symmetric and anti-symmetric stretching of P–O bond. The spectra of 2% Ce: LaPo4 and 6% Ce: LaPO4 also exhibit appropriate bands related to the conventional wave numbers [23]. As the overall transmittance reduces and when there is a shift towards the low wave number region, the doping effect could be the main cause. This is due to the variation in mass number of the dopant ions because the movement of mass of ions affects the structure and mechanical oscillations.

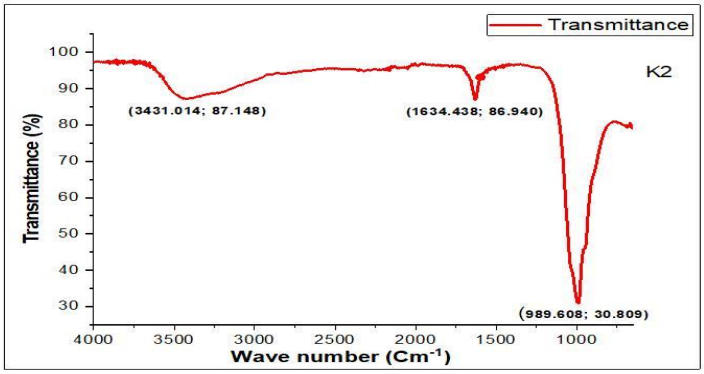

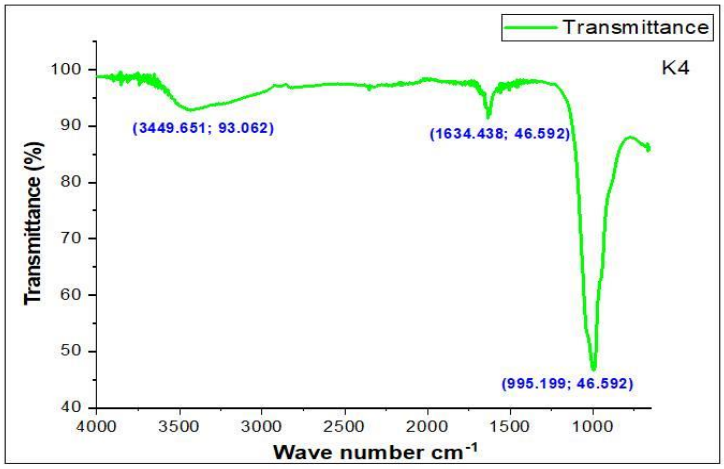

Fig 1.0 (a,b) FTIR spectra of 2% and 6% Ce:LaPO4

UV–VIS–spectroscopy:

UV spectroscopy is a powerful technique to analyze the electronic transition and optical band gap energy which is property of rare earth nanoparticles. Figure 2.0 (a,b) represents the UV–Vis absorption spectrum of LaPO4, 2% Ce: This was followed by 2% Ce:LaPO4 and then 6% Ce:LaPO4 phosphor samples [24], [25], [26]. When dopant ion cerium is added to pure lanthanum phosphate with varying dopant concentration of 2.0% only one peak appears at 367 nm as in figure 2.0 (a) for sample id K2 and when dopant ion cerium is added to pure lanthanum phosphate with varying dopant concentration of 6.0% also only one peak appears at 382 nm as in figure 2.0 Importantly, all peaks remain within the range of 200-800 nm. Furthermore, on doping the host (LaPO4) with cerium ion, the peaks found to be shifted towards the higher wavelength side (red shifted) [11], [27]. This technique also enables one to determine the electronic structure of the optical band structure of any material through UV–Visible absorption spectral analysis [28]. A transition from direct to indirect or vice versa and the optical band gap energy were computed with the help of Tauc's relation [29]. The energy band gap of material is determined by computing the square root of Ahv and by drawing a straight line through the linear region of the curve in fig 2.1 (a,b).The bandgap calculated for 2% cerium doped lanthanum phosphate is 3.55 eV and The bandgap calculated for 6% cerium doped lanthanum phosphate is 2.7 eV it indicate that material is more suitable for conduction, for absorbing a wider range of wavelengths including visible light. Lanthanum phosphate with varying dopant concentration of 2.0% only one peak appears at 367 nm as shown in fig 2.0 (a) with sample id K2, and when dopant ion cerium is added to pure lanthanum phosphate with varying dopant concentration of 6.0% also only one peak appears at 382 nm as shown in fig 2.0 (b) with sample id K4. All peaks lie in the range of 200-800 nm [30]. On doping the host (LaPO4) with cerium ion, the peaks are shifted towards longer wavelengths (red shift). UV–Visible absorption spectral study also helps one to find out the electronic structure of the optical band gap of material. The nature of transition (direct or indirect) and optical band gap energy were determined by Tauc's relation. The energy band gap of material can be obtained by plotting 〖(Ahv)〗^(1/2) versus energy and by extrapolating the linear portion of the curve as shown in fig 2.1 (a,b). The bandgap observed for 2% cerium doped lanthanum phosphate is 3.55eV and the bandgap observed for 6% cerium doped lanthanum phosphate is 2.7eV. This decrease

in band gap shows that the materials is more efficient for conduction and absorb a wide range of wavelength including visible light [31]. This decrease in band gap improves the opto-electronic application of these material and energy storage applications of these materials respectively [28], [32]. Material reduces the band gap by modulating the density of states. The doping technique has been commonly used to alter the host lattice's (LaP) electrical structure in order to produce new or enhanced optical characteristics that are advantageous from an application standpoint [33]. As a result, the optically dominant material 5% ofY:LaP, which has a band gap of 3.5 eV, can be utilized in conducting materials, high-performance luminous devices, and several optoelectronic device applications

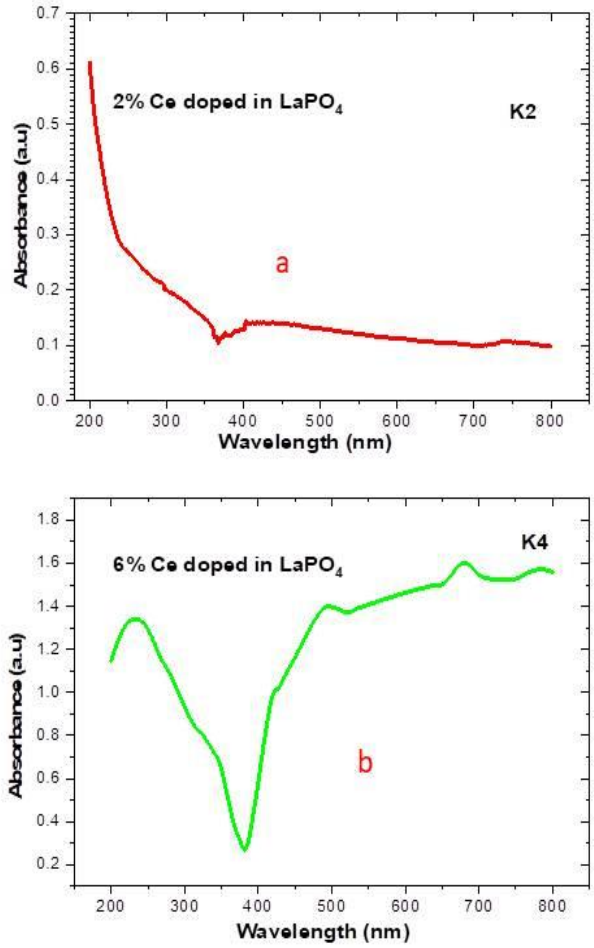

Fig 2.0 (a,b) UV-Visible Absorption Spectra of 2% and 6% Ce:LaPO4

The energy band gap of material can be obtained by plotting 〖(Ahv)〗^(1/2) versus energy and by extrapolating the linear portion of the curve as shown in fig 2.1 (a,b). The bandgap observed for 2% cerium doped lanthanum phosphate is 3.55eV and the bandgap observed for 6% cerium doped lanthanum phosphate is 2.7eV. This decrease in band gap shows that the material is more efficient for conduction, absorb a wide range of wavelength including visible light. This decrease in band gap enhanced optical properties and conductivity make these materials suitable for opto-electronic applications and energy storage applications respectively.

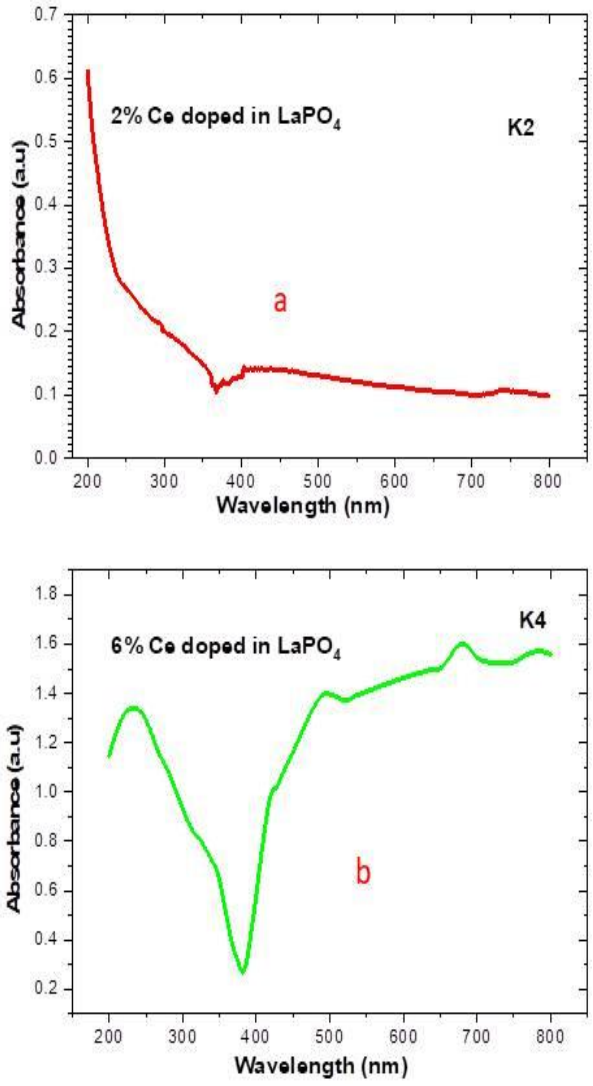

Fig 2.1 (a,b) Band gap of 2% and 6% Ce:LaPO4

Conclusion:

Ce:LaPO4 phosphor with different concentration such as 2.0 mol% and 6.0 mol% was successfully synthesized by using wet chemical co-precipitation method at low temperature. The photoluminescence study shows that the emissions of 367 nm are due to transition 5d4 □7f6, 382 nm due to 5d4□7f4 and 594 nm due to 5d4□7f5. The PL intensity is very high; hence the Ce :LaPO4 phosphors are applicable in various types of lamp and display devices. The method of synthesis used here is easy and economical, hence can be potentially applied for the synthesis of other high quality rare earth ions doped phosphate phosphor.

References

[1] J. X. Xu, Y. Yuan, S. Zou, O. Chen, and D. Zhang, "A Divide-and-Conquer Strategy for Quantification of Light Absorption, Scattering, and Emission Properties of Fluorescent Nanomaterials in Solutions," Anal Chem, vol. 91, no. 13, p. 8540, 2019.

[2] Z. J. Berkson et al., "Active Site Descriptors from 95Mo NMR Signatures of Silica-Supported Mo-Based Olefin Metathesis Catalysts," J Am Chem Soc, vol. 145, no. 23, p. 12651, 2023.

[3] B. Poornaprakash, U. Chalapathi, P. T. Poojitha, S. V. P. Vattikuti, and M. S. P. Reddy, "(Al, Cu) Co-doped ZnS nanoparticles: structural, chemical, optical, and photocatalytic properties," J. Mater. Sci. Mater. Electron., vol. 30, no. 10, pp. 9897–9902, May 2019, doi: 10.1007/s10854-019-01327-8.

[4] H. Nasrollahpour, B. J. Sánchez, M. Sillanpää, and R. Moradi, "Metal Nanoclusters in Point-of-Care Sensing and Biosensing Applications," ACS Appl Nano Mater, vol. 6, no. 14, p. 12609, 2023.

[5] B. Zhang, Y. Xu, J. Wang, J. Lin, C. Wang, and Y. Chen, "Lanthanum and cerium Co-doped LiFePO4: Morphology, electrochemical performance and kinetic study from −30 - +50 °C," Electrochimica Acta, vol. 322, p. 134686, Nov. 2019, doi: 10.1016/j.electacta.2019.134686.

[6] Y. Grynko and Y. Shkuratov, "Ray tracing sumulation of light scattering by spherical clusters consisting of particles with different shapes," J Quant Spectrosc Radiat, vol. 106, p. 56, 2007.

[7] M. S. P. Enders et al., "Characterization of Inorganic Solids Present in Brazilian Crude Oil Emulsions Using Scanning Electron Microscopy (SEM) with Energy-Dispersive X-ray Spectrometry (EDS): Evaluation of the Effect of Solvents," Energy Fuels, vol. 34, no. 2, pp. 1309–1316, Feb. 2020, doi: 10.1021/acs.energyfuels.9b03087.

[8] D. D. Andhare, S. A. Jadhav, M. V. Khedkar, S. B. Somvanshi, S. D. More, and K. M. Jadhav, "Structural and Chemical Properties of ZnFe2O4 Nanoparticles Synthesised by Chemical Co-Precipitation Technique," J. Phys. Conf. Ser., vol. 1644, no. 1, p. 012014, Oct. 2020, doi: 10.1088/1742-6596/1644/1/012014.

[9] M. S. H. Akash and K. Rehman, Essentials of Pharmaceutical Analysis. Singapore: Springer Nature Singapore, 2020. doi: 10.1007/978-981-15-1547-7.

[10] H. Z. Mahmood et al., "Plasmon-Based Label-Free Biosensor Using Gold Nanosphere for Dengue Detection," Crystals, vol. 11, no. 11, p. 1340, Nov. 2021, doi: 10.3390/cryst11111340.

[11] N. Abid et al., "Synthesis of nanomaterials using various top-down and bottom-up approaches, influencing factors, advantages, and disadvantages: A review," Adv. Colloid Interface Sci., vol. 300, p. 102597, Feb. 2022, doi: 10.1016/j.cis.2021.102597.

[12] A. Khan et al., "Cobalt/cerium-based ternary Prussian blue analogs as battery type electrode for supercapacitor applications," J. Alloys Compd., vol. 964, p. 171303, Nov. 2023, doi: 10.1016/j.jallcom.2023.171303.

[13] J. P. Horwath, D. N. Zakharov, R. Mégret, and E. A. Stach, "Understanding important features of deep learning models for segmentation of high-resolution transmission electron microscopy images," Npj Comput. Mater., vol. 6, no. 1, p. 108, Jul. 2020, doi: 10.1038/s41524-020-00363-x.

[14] H. M. Ali et al., "Advances in thermal energy storage: Fundamentals and applications," Prog. Energy Combust. Sci., vol. 100, p. 101109, Jan. 2024, doi: 10.1016/j.pecs.2023.101109.

[15] O. AitMellal et al., "Structural properties and near-infrared light from Ce3+/Nd3+-co-doped LaPO4 nanophosphors for solar cell applications," J. Mater. Sci. Mater. Electron., vol. 33, no. 7, pp. 4197–4210, Mar. 2022, doi: 10.1007/s10854-021-07615-6.

[16] N. A. Shad et al., "Fabrication of Spike-Like Spherical Iron Manganite Nanoparticles for the Augmented Photocatalytic Degradation of Methylene Blue Dye," J. Electron. Mater., vol. 51, no. 2, pp. 900–909, Feb. 2022, doi: 10.1007/s11664-021-09371-z.

[17] V. V. Deshmukh et al., "Enhanced multifunctional properties of lanthanum-doped barium ferrite nanoparticles synthesized via sol-gel assisted hydrothermal method," J. Energy Storage, vol. 82, p. 110559, Mar. 2024, doi: 10.1016/j.est.2024.110559.

[18] Burhanuddin et al., "Lanthanum doped hybrid LaxBi2−xSn2O7/SnO2(β-Bi2O3) nanostructures for energy storage applications," J. Alloys Compd., vol. 963, p. 171245, Nov. 2023, doi: 10.1016/j.jallcom.2023.171245.

[19] M. R. Razanajatovo, W. Gao, Y. Song, X. Zhao, Q. Sun, and Q. Zhang, "Selective adsorption of phosphate in water using lanthanum-based nanomaterials: A critical review," Chin. Chem. Lett., vol. 32, no. 9, pp. 2637–2647, Sep. 2021, doi: 10.1016/j.cclet.2021.01.046.

[20] N. A. Shad et al., "Zn3(VO4)2/Bi2WO6 composite based versatile platform for cotinine sensing and latent fingerprints development by using multiple modalities," Mater. Sci. Eng. B, vol. 301, p. 117203, Mar. 2024, doi: 10.1016/j.mseb.2024.117203.

[21] K. Vijayaraghavan and T. Ashokkumar, "Plant-mediated biosynthesis of metallic nanoparticles: A review of literature, factors affecting synthesis, characterization techniques and applications," J. Environ. Chem. Eng., vol. 5, no. 5, pp. 4866–4883, Oct. 2017, doi: 10.1016/j.jece.2017.09.026.

[22] K. M. Fahelelbom, A. Saleh, M. M. A. Al-Tabakha, and A. A. Ashames, "Recent applications of quantitative analytical FTIR spectroscopy in pharmaceutical, biomedical, and clinical fields: A brief review," Rev. Anal. Chem., vol. 41, no. 1, pp. 21–33, Jan. 2022, doi: 10.1515/revac-2022-0030.

[23] K. Candoğan, E. G. Altuntas, and N. İğci, "Authentication and Quality Assessment of Meat Products by Fourier-Transform Infrared (FTIR) Spectroscopy," Food Eng. Rev., vol. 13, no. 1, pp. 66–91, Mar. 2021, doi: 10.1007/s12393-020-09251-y.

[24] M. O. Guerrero-Pérez and G. S. Patience, "Experimental methods in chemical engineering: Fourier transform infrared spectroscopy—FTIR," Can. J. Chem. Eng., vol. 98, no. 1, pp. 25–33, Jan. 2020, doi: 10.1002/cjce.23664.

[25] N. Ž. Knežević, N. Ilić, V. Dokić, R. Petrović, and D. o. e. Janaćković, "Mesoporous Silica and Organosilica Nanomaterials as UV-Blocking Agents," ACS Appl Mater Interfaces, vol. 10, no. 24, p. 20231, 2018.

[26] C. B. Nettles, Y. Zhou, S. Zou, and D. Zhang, "UV-Vis Ratiometric Resonance Synchronous Spectroscopy for Determination of Nanoparticle and Molecular Optical Cross Sections," Anal Chem, vol. 88, no. 5, p. 2891, 2016.

[27] M. Nurjayadi, F. Romundza, and M. Moersilah, “Application of the Lambert-Beer legal concept in learning spectroscopy UV-Vis with simple spectrophotometers,” presented at the 2ND SCIENCE AND MATHEMATICS INTERNATIONAL CONFERENCE (SMIC 2020): Transforming Research and Education of Science and Mathematics in the Digital Age, Jakarta, Indonesia, 2021, p. 040009. doi: 10.1063/5.0041895.

[28] L. Kleine-Kleffmann, V. Stepanenko, K. Shoyama, M. Wehner, and F. Würthner, “Controlling the Supramolecular Polymerization of Squaraine Dyes by a Molecular Chaperone Analogue,” J Am Chem Soc, vol. 145, no. 16, p. 9144, 2023.

[29] N. Sivakumar, P. Nagaraju, A. Alsalme, A. Alghamdi, and R. Jayavel, “Enhanced electrochemical performance of lanthanum ferrite decorated reduced graphene oxide nanocomposite electrodes prepared by in situ microwave irradiation for energy storage applications,” Int. J. Energy Res., vol. 45, no. 4, pp. 5272–5282, Mar. 2021, doi: 10.1002/er.6146.

[30] J. Tauc, R. Grigorovici, and A. Vancu, “Optical Properties and Electronic Structure of Amorphous Germanium,” Phys Status Solidi B, vol. 15, no. 2, p. 627, 1966.

[31] M. W. Raza et al., “Strategy to enhance the electrochemical characteristics of lanthanum sulfide nanorods for supercapacitor applications,” J. Nanoparticle Res., vol. 23, no. 9, p. 207, Sep. 2021, doi: 10.1007/s11051-021-05307-0.

[32] Y. H. Fu, A. I. Kuznetsov, A. E. Miroshnichenko, Y. F. Yu, and B. Luk’yanchuk, “Directional visible light scattering by silicon nanoparticles,” Nat Commun, vol. 4, no. 1, p. 1527, 2013.

[33] A. Anantharaman, T. L. Ajeesha, JeenaN. Baby, and M. George, “Effect of structural, electrical and magneto-optical properties of CeMnxFe1-xO3-δ perovskite materials,” Solid State Sci., vol. 99, p. 105846, Jan. 2020, doi: 10.1016/j.solidstatesciences.2019.02.007.

[34] D. V. M. Arole and S. V. Munde, “FABRICATION OF NANOMATERIALS BY TOP-DOWN AND BOTTOM-UP APPROACHES – AN OVERVIEW,” vol. 1, no. 2, 2014.